Struct Multidisc Optim 22, 139–148

Minimal compliance fastening of elastic bodies

S.J. Cox and P.X. Uhlig

Abstract Permitted to fasten an elastic body on but half of its boundary, which portion should be fastened in order to minimize the work done by a specified load? For both plates and planar sheets we establish the existence of a unique solution to a relaxed version of the problem and present the results of a detailed numerical investigation.

Key words variable distributed support, planar elasticity, plates

1 Introduction

We determine the most effective way to fasten a body under a prescribed body force. By "fasten" we mean that material points on the boundary remain fixed during deformation. By "most effective" we mean that we minimize compliance, i.e. work done by the load. Although compliance minimization is a well developed subject (see e.g. Bendsøe 1995), the question of optimal support has received relatively little attention. The bulk, if not all, of the related work has sought the optimal placement of a finite number of lumped support mechanisms (see Bojczuk and Mroz 1998; Dekhtyar 1997; Dems and Turant 1997; Rozvany 1994; Wang *et al.* 1997; Rozvany 1974; Prager and Rozvany 1975; Mroz and Rozvany 1975). We believe this to be the first study to accommodate distributed fastening.

Received September 29, 2000
Communicated by J. Sobieski

S.J. Cox[1] and P.X. Uhlig[2]

[1] Department of Computational and Applied Mathematics, Rice University, Houston, TX 77251, USA
e-mail: `cox@rice.edu`
[2] Mathematics Department, St. Mary's University, San Antonio, TX 78228, USA
e-mail: `mathpaul@stmarytx.edu`

For the sake of exposition we work in two concrete contexts, namely planar sheets under in-plane loading and thin plates under transverse loading. In each case we establish existence and necessary conditions and obtain numerical results for a variety of shapes and loadings.

2 Planar elasticity

We suppose our body, Ω, to be an open, bounded, connected planar set with a smooth boundary, $\partial\Omega$. Under the action of a body force, f, points $x \in \Omega$ are deformed to $x + u(x)$. One encodes the resulting strain in

$$\varepsilon \equiv \begin{pmatrix} \varepsilon_{11} & \varepsilon_{12} \\ \varepsilon_{12} & \varepsilon_{22} \end{pmatrix} \equiv \begin{bmatrix} u_{1,1} & (u_{2,1}+u_{1,2})/2 \\ (u_{2,1}+u_{1,2})/2 & u_{2,2} \end{bmatrix} .$$

This strain induces a stress that, on supposing the body to be orthotropic with material symmetries across the x_1 and x_2 axes, takes the form

$$\sigma \equiv \begin{pmatrix} \sigma_{11} & \sigma_{12} \\ \sigma_{12} & \sigma_{22} \end{pmatrix} \equiv$$

$$\begin{pmatrix} \frac{E_1}{\mu}\varepsilon_{11} + \frac{E_1}{\mu}\nu_{21}\varepsilon_{22} & 2G\varepsilon_{12} \\ 2G\varepsilon_{12} & \frac{E_1}{\mu}\nu_{21}\varepsilon_{11} + \frac{E_2}{\mu}\varepsilon_{22} \end{pmatrix} ,$$

where

$$\mu = 1 - \nu_{21}^2 E_1/E_2 .$$

The stress, σ, must balance the body force, through

$$-\nabla \cdot \sigma = f , \tag{1}$$

while simultaneously accommodating any boundary conditions. In this regard we suppose the body to be fastened along $\Gamma \subset \partial\Omega$, i.e.

$$u = 0 \quad \text{on } \Gamma , \tag{2}$$

and traction free on its complement, i.e.

$$\sigma n = 0 \quad \text{on } \partial\Omega \setminus \Gamma\,. \tag{3}$$

For u satisfying (1) and (2)–(3) we denote the associated compliance by

$$\mathcal{C}(\Gamma) \equiv \int_\Omega f^T u \,\mathrm{d}x\,,$$

and record the variational characterization

$$\mathcal{C}(\Gamma) = \sup_{v \in H_\Gamma} P(v)\,, \tag{4}$$

where $H_\Gamma \equiv \{v \in H^1(\Omega)^2 : v|_\Gamma = 0\}$ is the class of kinematically admissible displacement fields and

$$P(v) \equiv 2\int_\Omega v^T f \,\mathrm{d}x - \int_\Omega \mathrm{tr}(\sigma^T \varepsilon)\,\mathrm{d}x$$

is the (negative of the) associated potential energy. We note that the supremum in (4) is indeed attained at the solution u to (1)–(3).

With these preliminaries out of the way we arrive at our main goal, the minimization of the compliance, $\mathcal{C}$, over those Γ of prescribed measure. More precisely, we shall consider the optimal design problem

$$\inf_{\Gamma \in ad_\gamma} \mathcal{C}(\Gamma) = \inf_{\Gamma \in ad_\gamma} \sup_{u \in H_\Gamma} P(u)\,. \tag{5}$$

where

$$ad_\gamma \equiv \{1_\Gamma : \Gamma \subset \partial\Omega,\ |\Gamma| = \gamma|\partial\Omega|\}\,.$$

Here $0 < \gamma < 1$ plays the role of length fraction, 1_Γ is the characteristic function of Γ, i.e.

$$1_\Gamma(x) = \begin{cases} 1 & \text{if} \quad x \in \Gamma\,, \\ 0 & \text{otherwise,} \end{cases}$$

and $|\Gamma|$ denotes the length of Γ. As stated, this design problem, (5), poses two obstacles. The first is that in the inner supremum the design variable lies not in the inner objective functional but rather deep in the definition of the class of kinematically admissible displacements. The second obstacle is that one can hardly expect the best fastener to be composed of a finite number of boundary arcs, instead, say based on the evidence gathered by Cox and Uhlig (1999), we expect the best fastener to be "smeared" along most if not all of the boundary.

In answer to the first obstacle we select a large scalar k and introduce the penalized functional

$$P_k(v, 1_\Gamma) \equiv P(v) + k\int_{\partial\Omega} 1_\Gamma |v|^2 \,\mathrm{d}s\,.$$

It follows that

$$\int_\Omega u_k^T f \,\mathrm{d}x = \mathcal{C}_k(\Gamma) = P_k(u_k, 1_\Gamma) = \sup_{v \in H^1(\Omega)^2} P_k(v, 1_\Gamma)\,, \tag{6}$$

where u_k satisfies (1) and

$$k 1_\Gamma u + \sigma n = 0 \quad \text{on } \partial\Omega\,. \tag{7}$$

Hence, mechanically, the penalization of P has the effect of replacing the rigid fastener along Γ with an elastic fastener of stiffness k.

The standard reply to the second obstacle is to relax the problem. We accomplish that here by replacing ad_γ with its weak* closure

$$ad_\gamma^* \equiv \left\{ \theta : 0 \le \theta(x) \le 1 \quad \text{a.e.} \quad \int_{\partial\Omega} \theta(s)\,\mathrm{d}s = \gamma|\partial\Omega| \right\}\,.$$

The criteria for a successful relaxation is that the relaxed problem admit a minimizer and that the value at the minimizer be no lower than the value of the unrelaxed infimum. Arguing precisely as Cox and Uhlig (1999, Cor. 2.3.), we may show that indeed

$$\inf_{1_\Gamma \in ad_\gamma} \mathcal{C}_k(1_\Gamma) = \min_{\theta \in ad_\gamma^*} \mathcal{C}_k(\theta)\,,$$

where, as suggested by (6), $\mathcal{C}_k(\theta)$ is the regularized compliance

$$\mathcal{C}_k(\theta) = \sup_{v \in H^1(\Omega)^2} P_k(v, \theta)\,. \tag{8}$$

As P_k is affine in θ and suprema of affine functions are convex it follows that $\mathcal{C}_k$ is convex and so every critical point is a minimizer. Regarding critical points we note that the gradient of $\mathcal{C}_k$ at θ is simply the gradient of $P_k(u, \cdot)$ at (u, θ) where u is the displacement associated with θ. That is

$$\langle \partial\mathcal{C}_k(\theta), \psi \rangle \equiv \lim_{t \to 0} \frac{\mathcal{C}_k(\theta + t\psi) - \mathcal{C}_k(\theta)}{t} =$$

$$-k\int_{\partial\Omega} \psi |u|^2 \,\mathrm{d}s\,, \tag{9}$$

where u satisfies (1) and

$$k\theta u + \sigma n = 0 \quad \text{on } \partial\Omega\,. \tag{10}$$

If $\hat\theta$ minimizes $\mathcal{C}_k$ over ad_γ^* then $\partial\mathcal{C}_k(\hat\theta) \in N_{ad_\gamma^*}(\hat\theta)$, the cone of normals to ad_γ^* at $\hat\theta$. This leads, precisely as in the paper by Cox and Uhlig (1999, §4), to the existence of Lagrange multipliers, $\lambda_1 \le 0$ and λ_2 for which $|\lambda_1| + |\lambda_2| > 0$ and

$$\int_\Omega \hat\theta(\lambda_1|\hat u|^2 + \lambda_2)\,\mathrm{d}x = \max_{0 \le \theta \le 1} \int_\Omega \theta(\lambda_1|\hat u|^2 + \lambda_2)\,\mathrm{d}x\,, \tag{11}$$

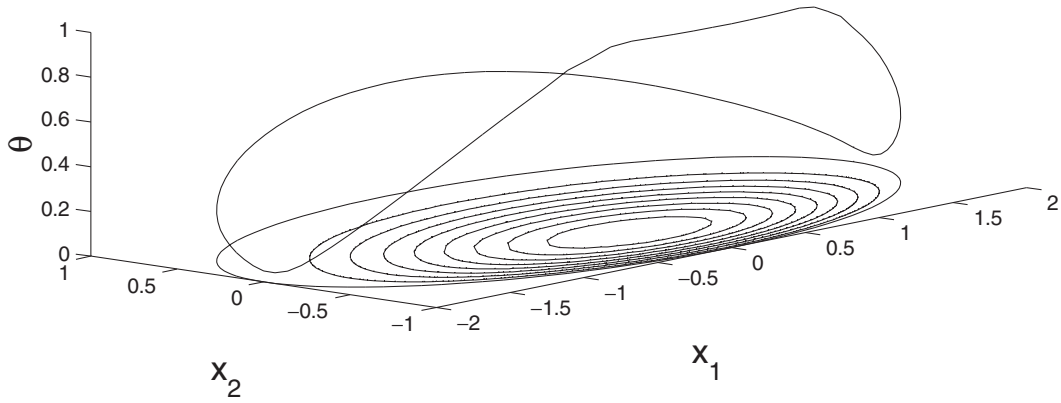

Fig. 1 Best θ for an isotropic ellipse with Young's moduli $E_1 = E_2 = 100$, Poisson's ratio $\nu_{21} = 0.3$, shear modulus $G = 38.46$, length fraction $\gamma = 0.5$, and fastener stiffness 10 000. The contours are level lines of the associated pointwise compliance, $u^T f$

where $\hat{u}$ is the displacement associated with $\hat{\theta}$. From $\lambda_1|\hat{u}|^2 \leq 0$ we deduce from (11) that $\lambda_2 > 0$. Similarly, $\lambda_1 < 0$. With $\lambda^2 \equiv -\lambda_2/\lambda_1$ we arrive at the pointwise necessary conditions

$$\hat{\theta}(x) = 0 \Rightarrow |\hat{u}(x)| \leq \lambda\,, \tag{12}$$

$$0 < \hat{\theta}(x) < 1 \Rightarrow |\hat{u}(x)| = \lambda\,, \tag{13}$$

$$\hat{\theta}(x) = 1 \Rightarrow |\hat{u}(x)| \geq \lambda\,. \tag{14}$$

It follows from (13) and (10) that where $\hat{\theta}$ is off of its bounds it must mirror the magnitude of the corresponding traction, i.e.

$$\hat{\theta} = \frac{1}{k\lambda}|\hat{\sigma}n|\,. \tag{15}$$

The centre condition, (13), is also natural in that it states that under optimal fastening no part of boundary suffers a larger motion than any other part. In other words, the minimal compliance fastener is an equi-fastener.

It is often the case that the optimality condition(s) overdetermine the equilibrium equations to such a degree that one can simply "read off" the form of the optimal design. In our case, if Ω is a disk centered at the origin subject to a radial body force then $\theta \equiv \gamma$ gives rise to a radial displacement field that indeed satisfies the optimality condition, (13).

In the nonradial case we must turn to numerical determination of the optimal design. For this purpose we have extended the algorithm of Cox and Uhlig (1999). We now discuss its application to the optimal fastening of isotropic and anisotropic ellipses subject to in-plane gravity. The associated body force is therefore

$$f(x) = \begin{bmatrix} 0 \\ -\ell(x) \end{bmatrix}\,,$$

where $\ell(x)$ is the vertical distance from x to the "top" of Ω. Applying such a load to an elliptical domain our optimization procedure returns the θ depicted in Fig. 1. As expected, θ is largest at the "bottom", where the body force is greatest, and smallest at the two "ends", where the boundary normal is orthogonal to the body force.

All computations were done in Matlab, using `constr` from the Optimization Toolbox and `assempde` from the Partial Differential Equations Toolbox. The corresponding finite element mesh was composed of 1500 vertices while the design variable, θ, was assumed constant on each of the 100 boundary segments.

In comparing Figs. 1 and 2b one sees that $|u|$ is indeed constant where θ is off its bounds and in excess of this constant where $\theta = 1$.

In the next sequence of plots we demonstrate the optimal fastening of the same ellipse under the same gravitational force but with an altered constitutive law. In particular, we suppose the directions of principal stretch to be $(1, -1)$ and $(1, 1)$ with distinct Young's moduli in the two directions.

Although Figs. 2 and 4 reveal a clear distinction between the isotropic and anisotropic displacements, the plots of the associated optimal fasteners in Figs. 1 and 3 appear quite similar. As an aid to discrimination we plot them side by side in Fig. 5.

Regarding extensions and limitations of our analyses, we have worked on planar problems solely out of computational convenience – our numerical engine, Matlab's PDE toolbox, is at present limited to second order operators in two spatial variables. Our existence result and necessary conditions remain valid in higher dimensions. Similarly, our consideration of linear rather than nonlinear elasticity has been one of convenience. The existence theory requires only hyperelasticity while the necessary conditions remain unchanged so long as there continues to exist a unique deformation, u. The case of multiple equilibria is similar to the case of multiple eigenvalues and so the compliance may be differentiated along the lines of Cox (1995).

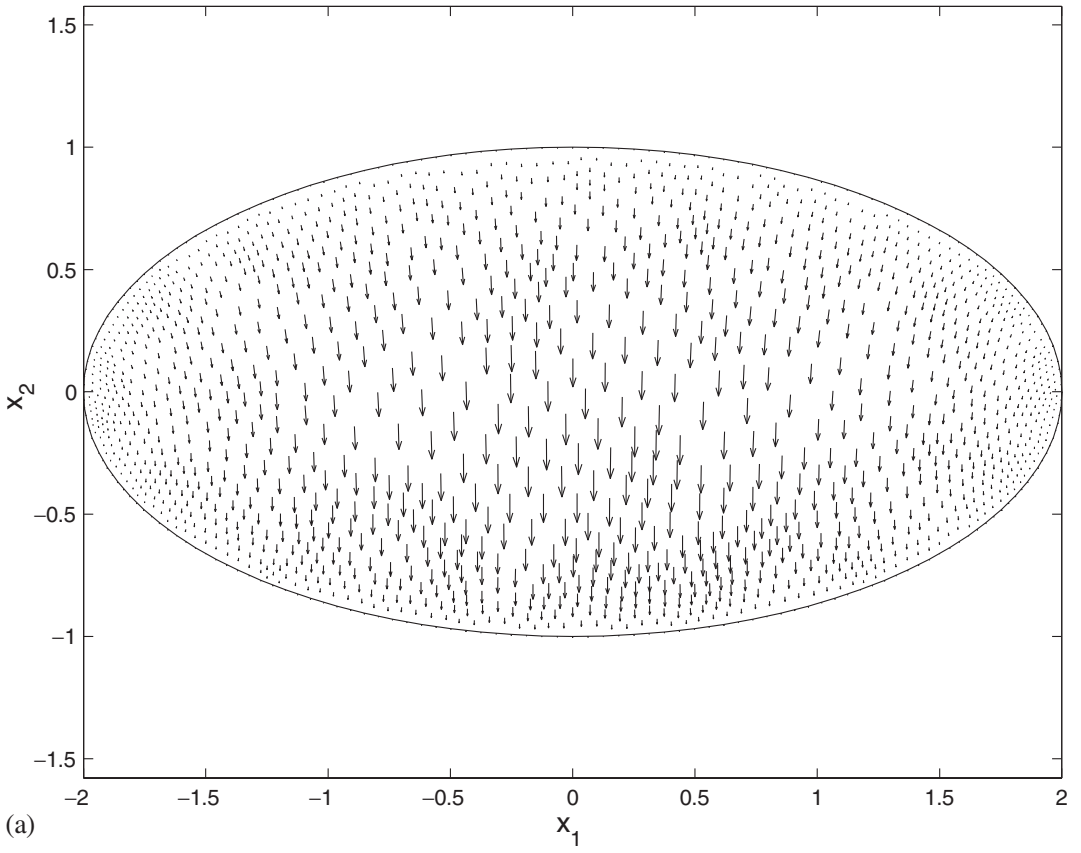

(a)

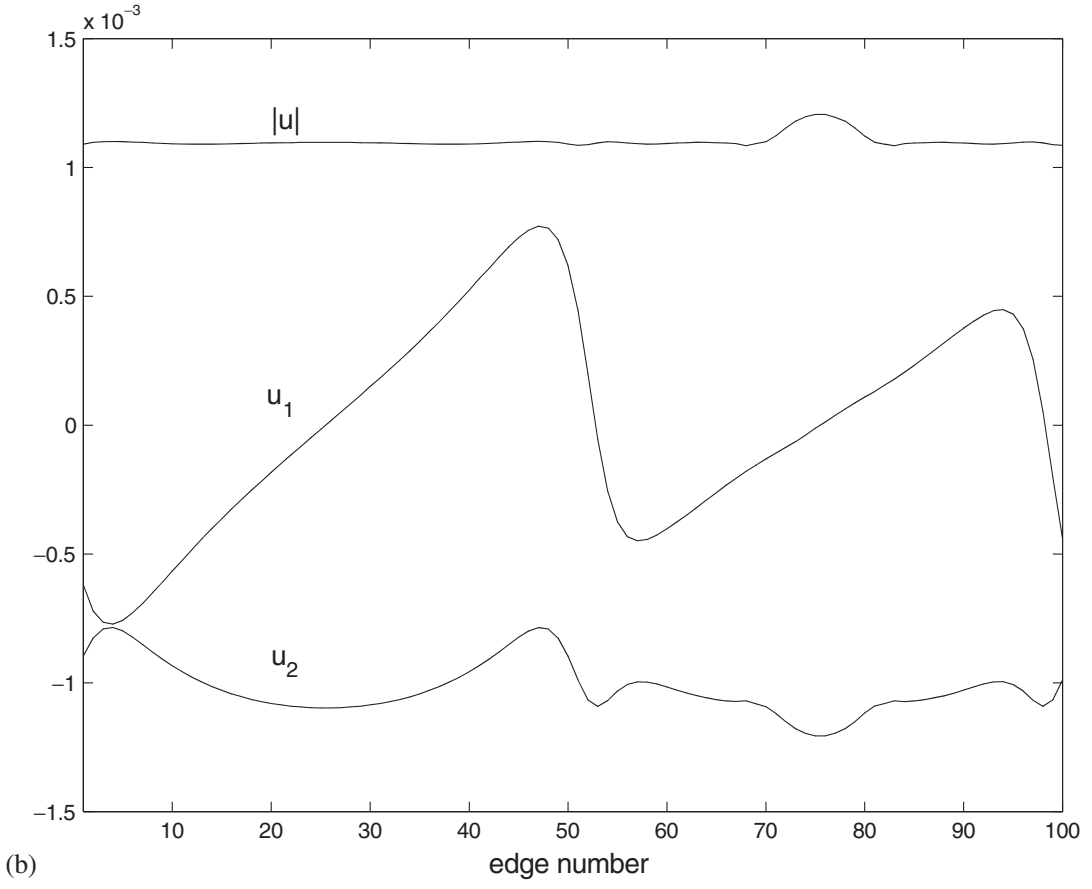

(b)

Fig. 2 (a) The displacement field associated with the θ of Fig. 1; (b) boundary values of the horizontal, u_1, vertical, u_2, and total, $|u|$, displacements associated with the θ of Fig. 1

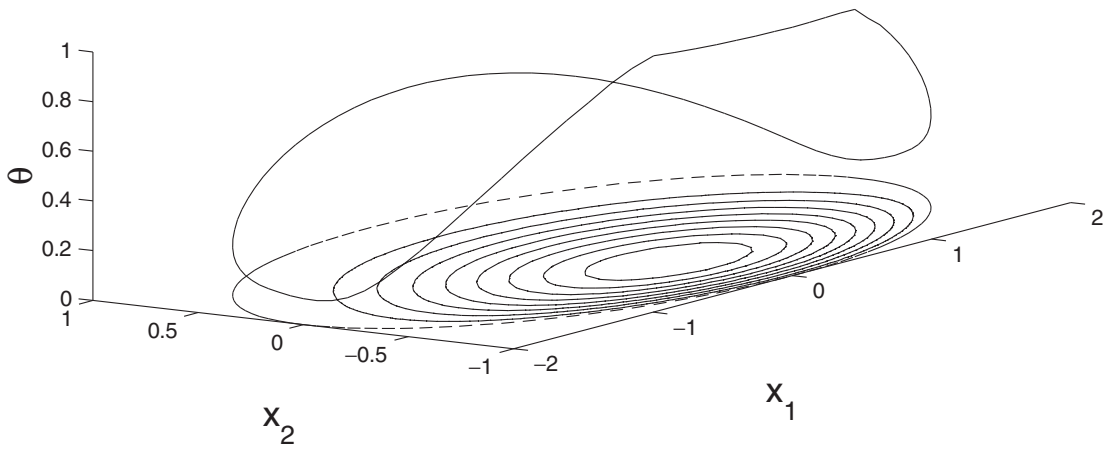

Fig. 3 Best θ for an anisotropic ellipse with Young's moduli $E_1 = 50$, $E_2 = 150$, Poisson's ratio $\nu_{21} = 0.3$, shear modulus $G = 42.62$, length fraction $\gamma = 0.5$, and fastener stiffness $k = 10\,000$. The contours are level lines of the associated pointwise compliance, $u^T f$

3 Plates

We now turn our attention to the optimal fastening of plates. For the sake of exposition we invoke the simplest, biharmonic, model and consider only one of the many types of possible fastenings. In particular, we seek the optimal clamping, i.e. we consider

$$\Delta^2 w = g \quad \text{in } \Omega\,, \qquad w = \partial w/\partial n = 0 \quad \text{on } \Gamma\,,$$

and seek to minimize the compliance

$$\int_\Omega wg\,\mathrm{d}x$$

over $\Gamma \in ad_\gamma$. The relaxed version has the form

$$\mathcal{C}_k(\theta) = \max_{z \in H^2(\Omega)} P_k(z,\theta)\,,$$

where the penalized potential energy is

$$P_k(z,\theta) = 2\int_\Omega zg\,\mathrm{d}x - \int_\Omega (\Delta z)^2\,\mathrm{d}x -$$

$$k\int_{\partial\Omega} \theta\{z^2 + (\partial z/\partial n)^2\}\,\mathrm{d}s\,.$$

Critical points of $P_k(\cdot,\theta)$ satisfy

$$\Delta^2 w = g \quad \text{in } \Omega\,, \tag{16}$$

$$k\theta w - \frac{\partial \Delta w}{\partial n} = 0 \quad \text{on } \partial\Omega\,, \tag{17}$$

$$\Delta w + k\theta \frac{\partial w}{\partial n} = 0 \quad \text{on } \partial\Omega\,. \tag{18}$$

The gradient of the compliance is

$$\langle \partial\mathcal{C}_k(\theta), \psi\rangle = -k\int_{\partial\Omega} \psi\{w^2 + (\partial w/\partial n)^2\}\,\mathrm{d}s\,, \tag{19}$$

where w is the displacement associated with θ. Arguing then as in the previous section we arrive at the following pointwise optimality conditions for the optimal fastener, $\hat\theta$, and its associated displacement, $\hat w$,

$$\hat\theta(x) = 0 \Rightarrow \hat w^2 + (\partial\hat w/\partial n)^2 \le \lambda\,, \tag{20}$$

$$0 < \hat\theta(x) < 1 \Rightarrow \hat w^2 + (\partial\hat w/\partial n)^2 = \lambda\,, \tag{21}$$

$$\hat\theta(x) = 1 \Rightarrow \hat w^2 + (\partial\hat w/\partial n)^2 \ge \lambda\,. \tag{22}$$

As above, these permit us to see that the constant fastener is the best fastener of a circular plate under a radial transverse load. Regarding more general shapes and loads we note that as (16)–(18) may be written as the second-order system

$$\Delta w_1 = w_2\,, \quad \Delta w_2 = g\,,$$

$$\frac{\partial w_1}{\partial n} + \frac{1}{k\theta} w_2 = 0\,, \quad \frac{\partial w_2}{\partial n} - k\theta w_1 = 0\,,$$

we may apply our aforementioned optimization algorithm. As our first example we consider an elliptical plate under a uniform load. We find confirmation of the optimality conditions, (20)–(22), in Fig. 7. For our next two examples we contrast the optimal fastenings of a square plate subject to uniform and concentrated loads. As for the ellipse, the optimal fastener devotes almost all of its resources to the long exposed edges.

Comparing Figs. 8 and 9 we see at once how the optimal fastener is attuned to the respective load. For our

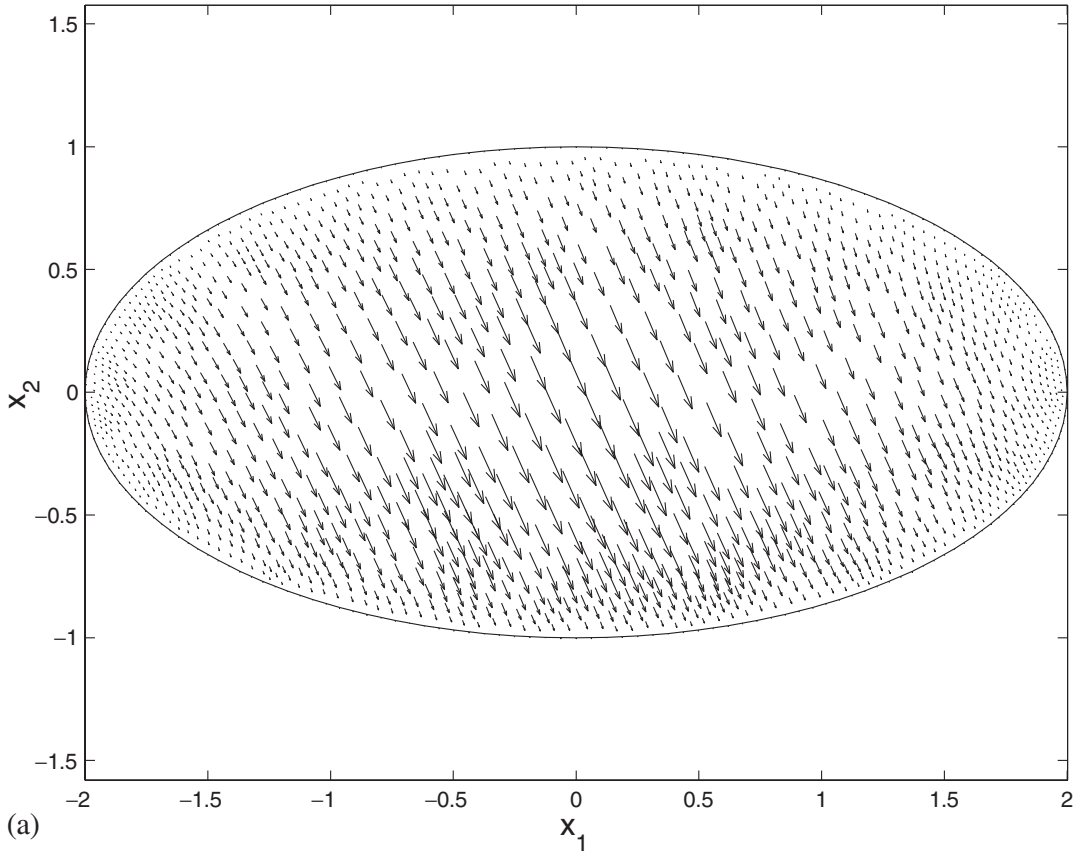

(a)

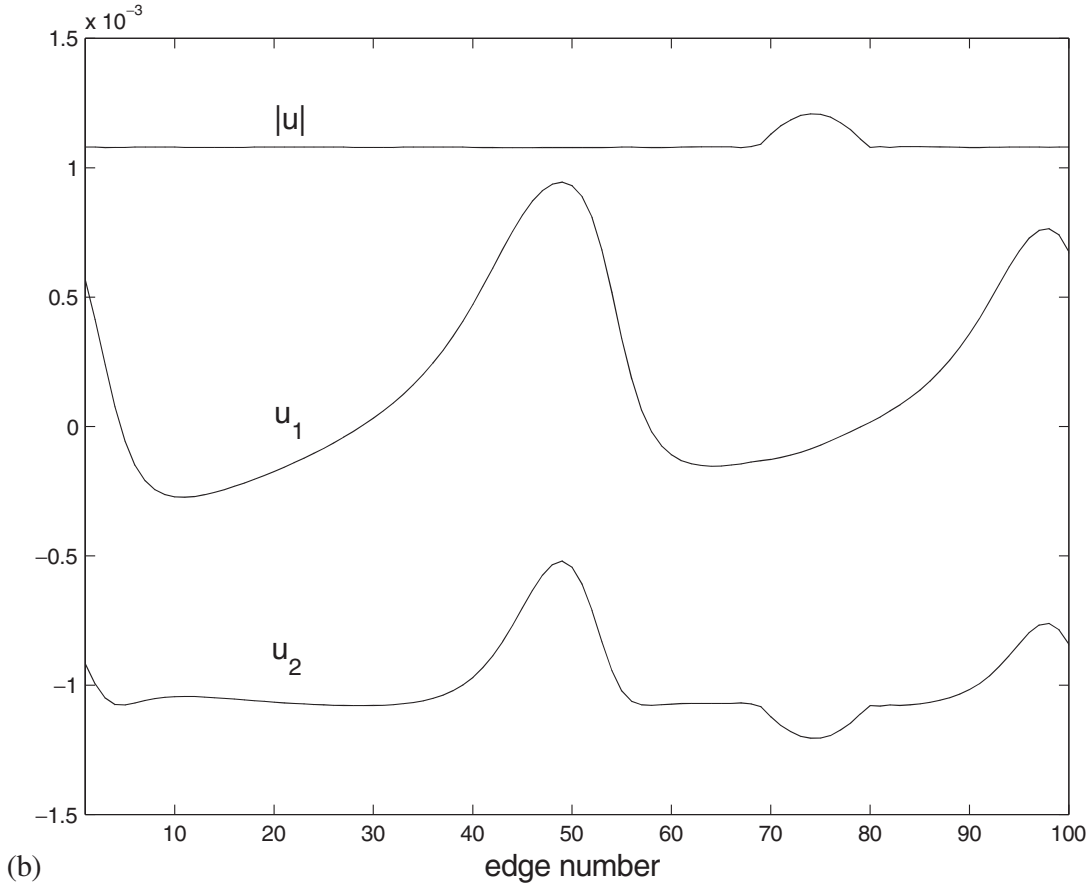

(b)

Fig. 4 (a) The displacement field associated with the θ of Fig. 3; (b) boundary values of the horizontal, u_1, vertical, u_2, and total, $|u|$, displacements associated with the θ of Fig. 3

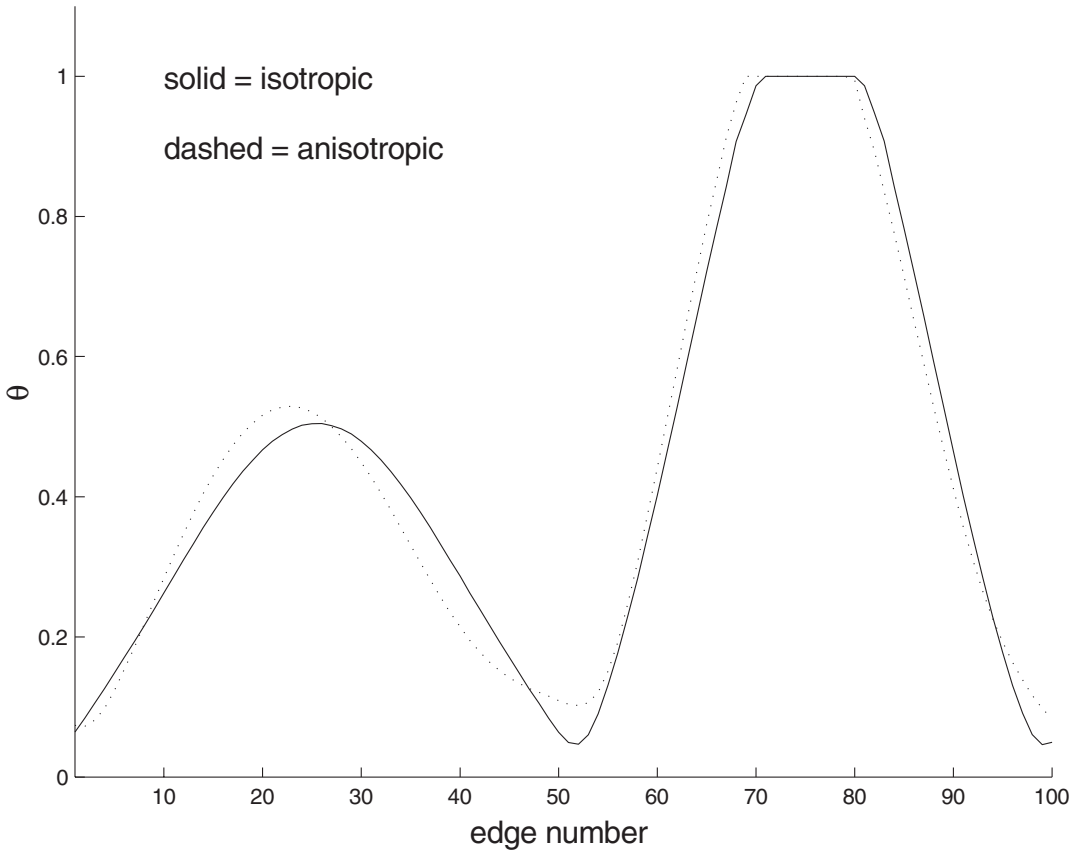

Fig. 5 Comparison of best isotropic and anisotropic fasteners

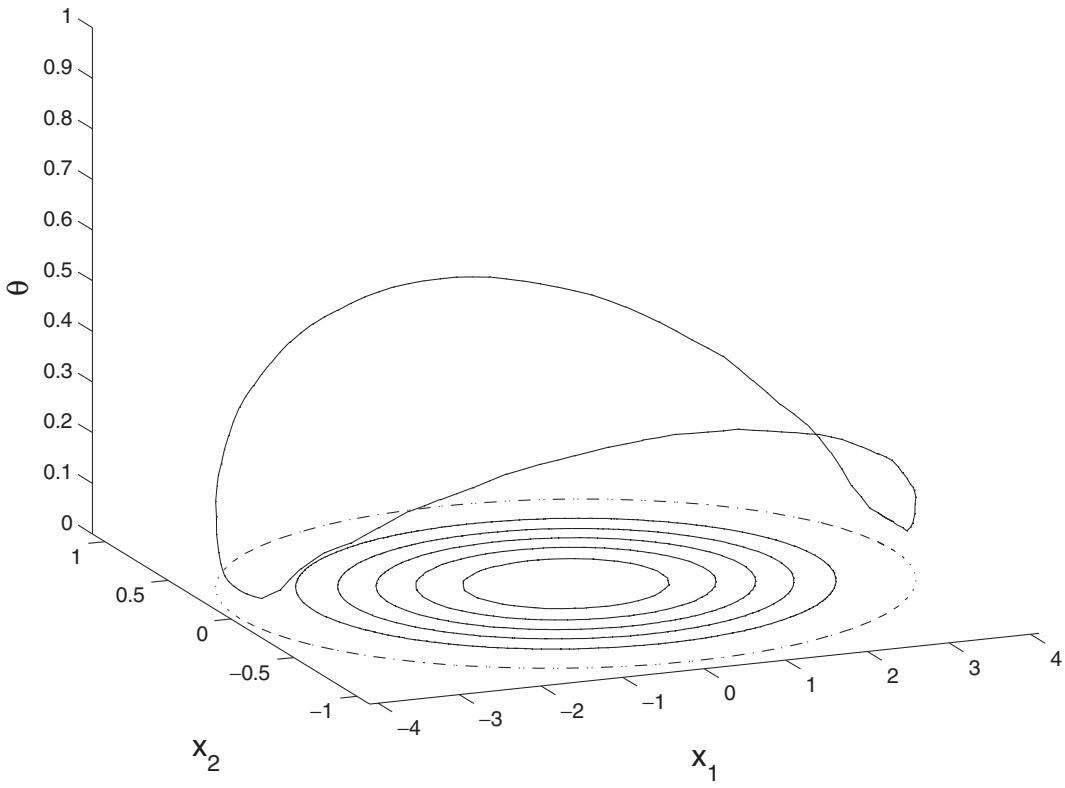

Fig. 6 Optimal clamping of an elliptical plate with $g \equiv 1$, $\gamma = 1/3$ and $k = 1000$. The contours are level lines of the associated displacement

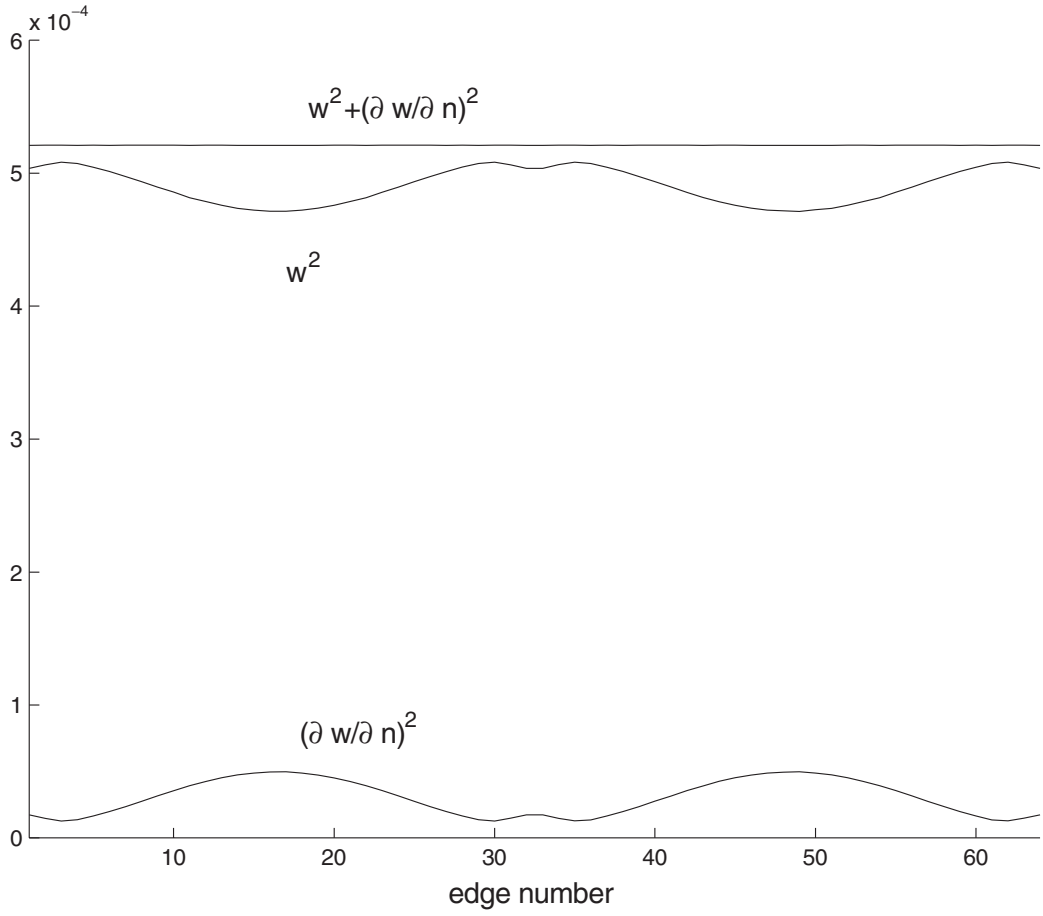

Fig. 7 The associated edge displacement and normal

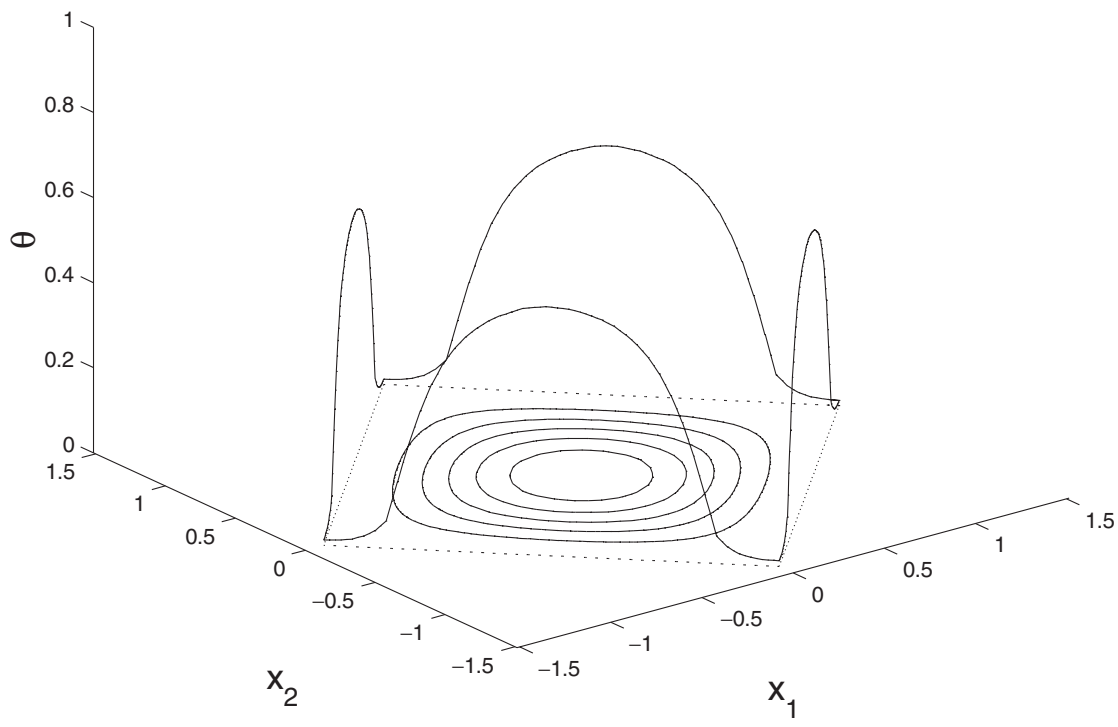

Fig. 8 Optimal clamping of a square plate with $g \equiv 1$, $\gamma = 1/3$ and $k = 1000$. The contours are level lines of the associated displacement

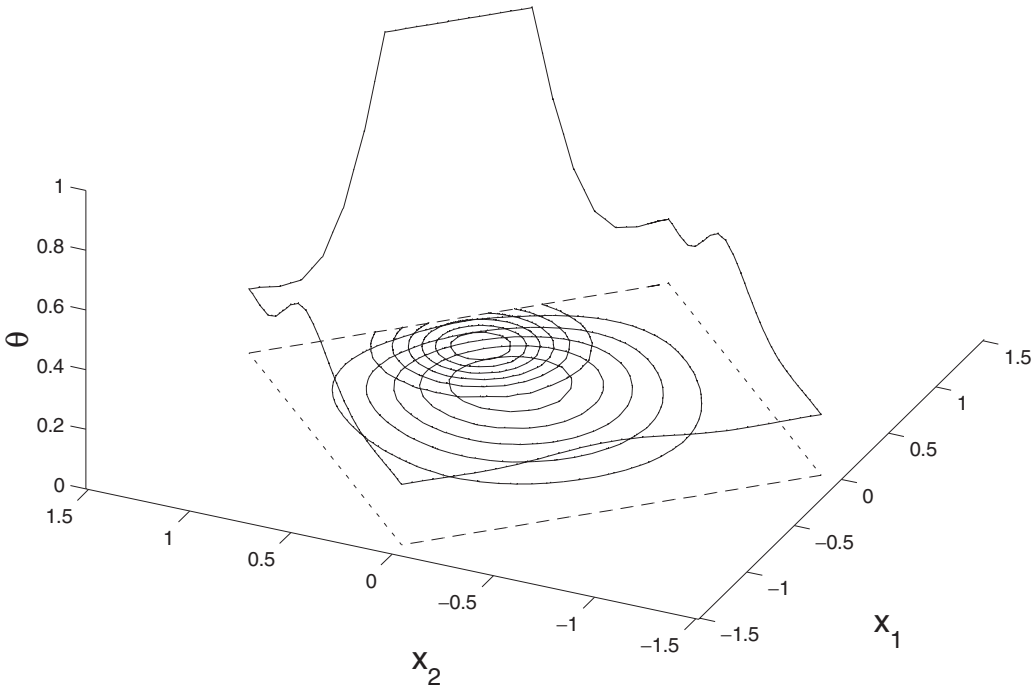

Fig. 9 Optimal clamping of a square plate with $g(x) = 4\exp(-8|x-(0.5,0.5)|^2)$, $\gamma = 1/3$ and $k = 1000$. The larger contours, centered near the plate's center, are level lines of the associated displacement. The smaller contours, centered near a side, are contours of the load, g

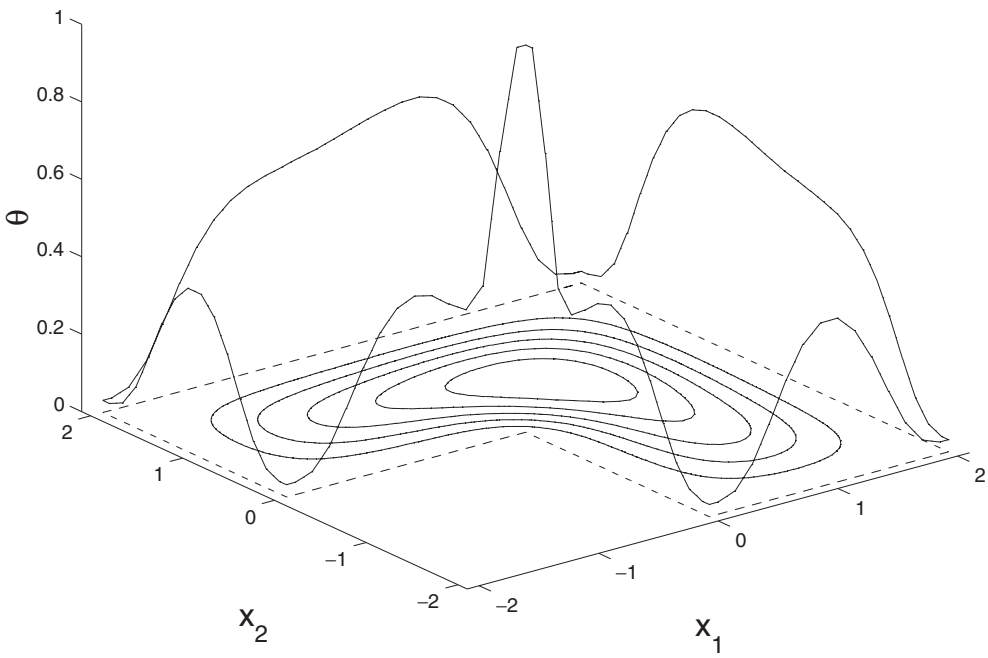

Fig. 10 Optimal clamping of an L-shaped plate with $g = 1$, $\gamma = 1/3$ and $k = 1000$. The contours are level lines of the associated displacement

final example we contrast optimal fastening at convex and concave corners. In the convex case we have seen that little to no fastening is needed while in the concave case, see Fig. 10, it is just the opposite. As stated at the close of the previous section, our formulation is robust enough to accommodate nonlinear, heterogeneous, anisotropic plates.

References

Bendsøe, M.P. 1995: *Optimization of structural topology, shape, and material.* Berlin, Heidelberg, New York: Springer

Bojczuk, D.; Mroz, Z. 1998: On optimal design of supports in beam and frame structures. *Struct. Optim.* **16**, 47–57

Cox, S.J. 1995: The generalized gradient at a multiple eigenvalue. *J. Functional Analysis* **33**, 30–40

Cox, S.J.; Uhlig, P.X. 1999: Where best to hold a drum fast. *SIAM J. Optimiz.* **9**, 948–964

Dekhtyar, A.S. 1997: Optimal point support of shells and plates. *Int. Appl. Mech.* **33**, 316–319

Dems, K.; Turant, J. 1997: Sensitivity analysis and optimal design of elastic hinges and supports in beam and frame structures. *Mech. Struct. Mach.* **25**, 417–443

Mroz, Z.; Rozvany, G.I.N. 1975: Optimal design of structures with variable support conditions. *J. Optimiz. Theory Appl.* **15**, 85–101

Prager, W.; Rozvany, G.I.N. 1975: Plastic design of beams: optimal locations of supports and steps in yield moment. *Int. J. Mech. Sci.* **17**, 627–631

Rozvany, G.I.N. 1974: Optimization of unspecified generalized forces in structural design. *J. Appl. Mech. (ASME)* **41**, 1143–1145

Rozvany, G.I.N. 1994: Optimal layout of grillages: allowance for the cost of supports and optimization of support locations. *Mech. Struct. Mach.* **22**, 49–72

Wang, C.M.; Xiang, Y.; Kitipornchai, S. 1997: Optimal locations of point supports in laminated rectangular plates for maximum fundamental frequency. *Struct. Eng. Mech.* **5**, 691–704